Sigma J Eng Nat Sci, Vol. 42, No. 2, pp. 503−515, April, 2024

Sigma Journal of Engineering and Natural Sciences
Web page info: https://sigma.yildiz.edu.tr
DOI: 10.14744/sigma.2022.00082

Research Article

Modeling and analysis of schottky diode bridge and JFET based liénard oscillator circuit

Kübra ÇAKIR[1,*], Reşat MUTLU[1]

[1]*Department of Electronics and Communication Engineering, Tekirdag Namik Kemal University, Tekirdag, 59500, Türkiye*

ARTICLE INFO

Article history
Received: 22 February 2022
Revised: 29 March 2022
Accepted: 05 June 2022

Keywords:
Liénard Oscillator; Schottky Diode Bridge; Chua Diode; Limit Cycle; Circuit Dynamics

ABSTRACT

Liénard Oscillator circuit has numerous variations. Nowadays, due to the developments of semiconductor technology, such an oscillator can be made using various semiconductor circuit elements. In this study, it has been shown that a Liénard Oscillator can also be made using a Schottky diode bridge and a JFET based nonlinear resistor. First, the new Liénard Oscillator topology is given, then, the dynamic model of the circuit is derived, and the simulations of the circuit are made. The currents, voltages and limit cycle of the Liénard Oscillator circuit are obtained with simulations using LTspice circuit analysis program. The simulations have confirmed that the circuit operates as a Liénard Oscillator.

Cite this article as: Çakır K, Mutlu R. Modeling and analysis of schottky diode bridge and JFET based liénard oscillator circuit. Sigma J Eng Nat Sci 2024;42(2):503−515.

INTRODUCTION

The Van Der Pol Oscillator (VDPO), which has been made in 1920 using a triode vacuum tube [1], is a widely known and studied oscillator. The stable oscillations which has been found in the triode circuit are called relaxation-oscillations by Van der Pol and its operation is explained in [2]. The frequency demultiplication phenomenon reported in this circuit is an example of deterministic chaos [3]. Historically, its discovery has helped to improve the nonlinear theory of oscillators [4]. Liénard's equations were proposed by the French physicist Alfred-Marie Liénard in 1928 to model oscillating circuits [5]. The Van der Pol Oscillator is modeled by the Van der Pol equations and the Liénard equations define the VDPO as a special case [5]. There are many articles written on the Liénard Oscillator or its equation. Liénard System can be and has been applied in various fields such as chemical reactions, radio and vacuum tube technology, electronic oscillators, lasers, predator-prey systems, growth of a single species, aortic blood flow, vibration analysis, etc. [6–9]. When the Van der Pol Oscillator or the Liénard Oscillator emerged, the semiconductor circuit elements were not yet available, but, today, a Liénard Oscillator can be implemented by using different types of semiconductor circuit elements such as the ones given in [10–12].

In [10], a hybrid optoelectronic integrated circuit with a resonant tunnelling diode driving an optical communications laser diode is shown to operate as a voltage-controlled oscillator with optical and electrical outputs and its operation is described by Liénard's equation. Even the new found nonlinear memristor element can be used in well-known

***Corresponding author.**
*E-mail address: kubracakir1999@gmail.com

This paper was recommended for publication in revised form by Regional Editor N. Özlem Ünverdi

Liénard systems and its behaviour is explored considering hidden attractors, different transitions of mixed-mode oscillations, higher dimensional torus, and large expanded strange attractor in [11]. In [12], it has been recently shown that a reverse-parallel Schottky diode array-based VDPO can be done deriving the circuit's differential equation and its waveforms and limit cycle are examined using simulations with not only Simulink but also LTspice. The Liénard equations often do not have exact solutions however it is sometimes possible for such a solution to exist. For example, Liénard type equations are solved using Sundman transform theory in [13] and the exact and explicit general harmonic and isochronous solutions have been possible for a special Liénard equation of the Van der Pol-Helmholtz Oscillator given in [14] and it is also shown that the analytical results obtained by the method used match the numerical results. The periodic orbits of a nonlinear VDPO are shown to exhibit the unexpected property that the frequency of oscillations is completely independent as if a linear harmonic oscillator in [15]. Sufficient conditions for the synchronization of coupled Liénard type oscillators are investigated using the averaging technique for a fixed, nonsymmetric, and nonlinear coupling and it is shown that the solutions of oscillators converge arbitrarily close to each other in [16] Some Liénard–Van der Pol Oscillators may have more than one limit cycles and this has been investigated in [17]. The nonlinear dynamics and active control of a Liénard type oscillator under parametric and external excitations are investigated and it is found that for an appropriate value of the control gain parameter, the chaotic behaviour can be completely removed of the system in [18]. The classical quantization of a Liénard type nonlinear oscillator is carried out by a quantization scheme that preserves the Noether point symmetries of the underlying Lagrangian in order to construct the Schrödinger equation [19]. In [20], a family of second order damped nonlinear oscillators, which generalizes the Liénard equation, is discussed. In [21], the quantum versions of Rayleigh, Van der Pol, and several other variants of Liénard Oscillators are derived as special cases. In [22], a PT-symmetric Liénard Oscillator configuration is investigated for two nonlinear power consumption cases. Due to these characteristics, modeling ability, and possible application areas such as synchronization and chaos, it is important to make and examine new types of VDPO and Liénard oscillators which can be possibly used in oscillator and chaos studies.

In [23], a Chua diode is obtained by using a Schottky diode bridge and a JFET-based negative resistance converter circuit, and this Chua diode is used in the construction of a Chua circuit. In [23], the Schottky diode bridge feeding the JFET is used to obtain the odd current-voltage characteristic required for the Chua's diode easily. Such a characteristic is also needed to make a VDPO and a Liénard Oscillator and it is a cheap solution since it uses off-the shelves and easy to find components. To the best of our knowledge, there is not a Liénard Oscillator made using a Chua diode consisting of a JFET and Schottky diode bridge yet. In this study, the nonlinear circuit element required for the Liénard Oscillator is made by connecting a linear resistor in parallel with a negative resistance converter circuit consisting of an op-amp, two linear resistors and a JFET fed with a Schottky diode bridge. The new Liénard Oscillator circuit is formed by connecting an inductor and a capacitor in parallel to this proposed nonlinear resistor. Such a circuit is made with easy to find, cheap, and off-the shelves circuit components. The circuit uses less diodes than the one given in [12]. In this study, it is also to be shown that the Schottky diode bridge provides an easy solution to make the odd function required for a Liénard Oscillator. The equations of the Liénard Oscillator are derived and it is simulated in LTspice™.

This study is organized in the following order. In the second section, basic information on Liénard Equation and Equation System is given. In the third section, Schottky diode bridge and JFET-based Liénard Oscillator circuit proposed in this study is given its working principle is explained. In the fourth section, it is shown that this oscillator is a Liénard Oscillator using differential equations. In the fifth section, the simulation results of this Liénard Oscillator circuit obtained with the LTspice program are given. The paper is concluded with the last section.

LIÉNARD EQUATION AND SYSTEM OF EQUATIONS

In this section, first the generic Liénard Equation and the Liénard System Equations are given and summarized.

Liénard's Equation

The Liénard System is named after the French physicist Alfred-Marie Liénard. This dynamical system is modeled by the Liénard equation, which is a second-order differential equation [5]. The Liénard equation has been used to model oscillating circuits during the development of radio and vacuum tube technology [5,20]. Liénard's Theorem proves the uniqueness and existence of the limit cycle in these systems or oscillators [5]. The definition of Liénard's equation can be given as: Let $f(x)$ be an even function and $g(x)$ an odd function, two continuously differentiable functions on R, which is the set of real numbers. In this case, the quadratic differential equation given below is called the Liénard equation:

$$\frac{d^2x}{dt^2} + f(x)\frac{dx}{dt} + g(x) = 0 \tag{1}$$

Van der Pol Oscillator which is a special case of the Liénard equation and is defined as

$$\frac{d^2V}{dt^2} - \frac{a}{C}(1 - V^2)\frac{dV}{dt} + \frac{1}{LC}V = 0 \tag{2}$$

Liénard System

The Liénard equation can be converted into an equivalent two-dimensional system of ordinary differential equations. Let's define

$$F(x) = \int_0^x f(\xi)d\xi \tag{3}$$

$$x_1 \coloneqq x$$

$$x_2 \coloneqq \frac{dx}{dt} + F(x) \tag{4}$$

Then, the following system is defined as the Liénard System:

$$\begin{bmatrix} \dot{x}_1 \\ \dot{x}_2 \end{bmatrix} = \mathbf{h}(x_1, x_2) \coloneqq \begin{bmatrix} x_2 - F(x_1) \\ -g(x_1) \end{bmatrix} \tag{5}$$

Since the Liénard equation is itself an autonomous differential equation, by defining the variable,

$$v = \frac{dx}{dt} \tag{6}$$

The Liénard equation can also alternatively be written as a first-order differential equation:

$$v\frac{dv}{dx} + f(x)v + g(x) = 0 \tag{7}$$

Liénard's Theorem

If a Liénard System meets the following criteria, it has a unique and stable limit cycle surrounding the origin.

- $g(x) > 0$ for all $x > 0$ values;
- For $0 < x < p$ and when $F(x) > 0$,
- $F(x)$ possess only a positive root, whose value is equal to p where $F(x) < 0$ for $0 < x < p$ and the function is monotonic and $F(x) > 0$ for $x > p$
- $\lim_{x\to\infty} F(x) := \lim_{x\to\infty} \int_0^\infty f(\xi)d\xi = \infty$;

GENERIC LIÉNARD OSCILLATOR CIRCUIT AND SCHOTTKY DIODE BRIDGE AND JFET BASED LIÉNARD OSCILLATOR

In this section, first the generic Liénard Oscillator is summarized and then the Liénard Oscillator circuit proposed in this study is introduced.

Overview of the Liénard Oscillator Circuit

The Van der Pol Oscillator consists of an inductor, a capacitor, and a nonlinear resistor. Since the Van der Pol Oscillator equation is a special case of the Liénard equation, it is also true that the Liénard Oscillator consists of an inductor, a capacitor, and a nonlinear resistor. The general (generic) Liénard Oscillator or Van der Pol Oscillator Circuit can be seen in Figure 1 [12].

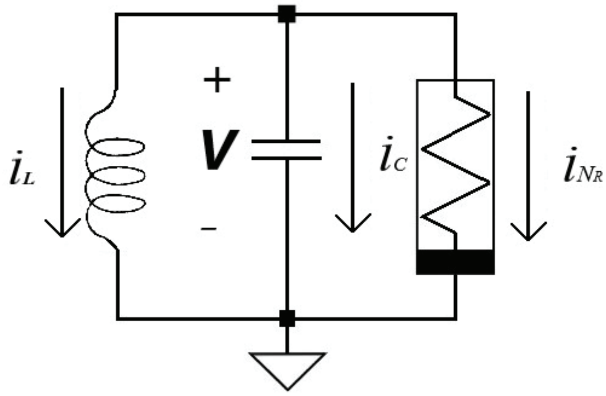

Figure 1. The generic Liénard Oscillator or the generic Van der Pol Oscillator circuit [12].

Investigation of Nonlinear Resistance of Liénard Oscillator Used in This Study and Liénard Circuit

As mentioned before, a nonlinear resistor must be used in the Liénard Oscillator. The Liénard Oscillator used in this study consists of a nonlinear resistor whose nonlinear resistance is an even function of voltage, a negative resistor converter circuit, and a linear time invariant resistor. Since a negative resistance feature is also required in nonlinear resistance, an op-amp based negative resistance converter circuit is used. The negative resistance converter shown in Figure 2 acts as an active source, as it powers the circuit locally. This nonlinear resistor consists of a JFET fed with a Schottky diode bridge and a linear resistor (R_p) connected in parallel with it.

In Figure 3, the nonlinear resistor circuit used in this study in the place of the resistor R_2 seen in Figure 2 is given. The resistor R_p in the Chua diode voltage seen in Figure 3 is used to obtain the slope m_0 if the absolute value of

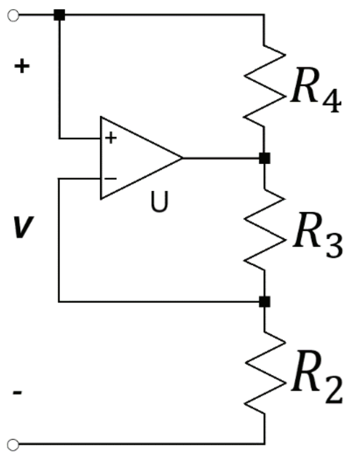

Figure 2. An op-amp based negative resistance converter circuit.

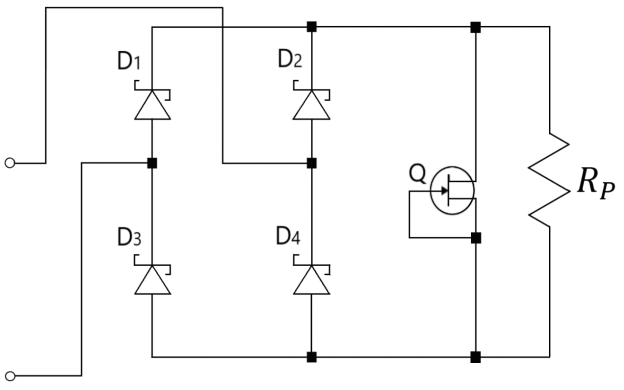

Figure 3. The nonlinear resistor circuit used instead of the resistor R_2 given in Figure 2.

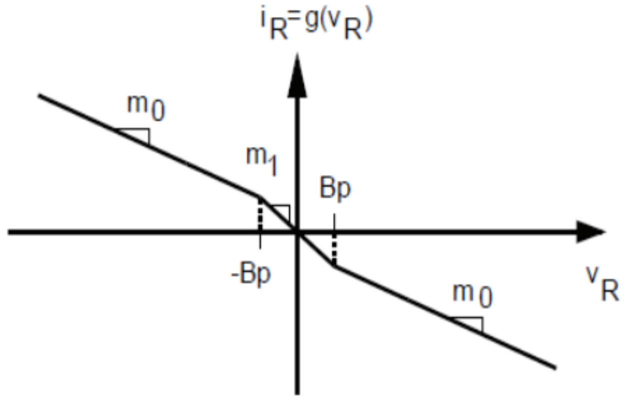

Figure 5. The v-i characteristic of a PWL Chua diode with three pieces [24].

its voltage is higher than the breakpoint voltage, B_P. The advantageous features of JFETs compared to BJTs are that they are voltage-controlled and operate with less noise than BJTs, and are smaller in size. For these reasons, an n-type BF245B type JFET is used in this study.

In Figure 4, the Schottky diode bridge and the JFET based Liénard Oscillator is shown. The negative nonlinear resistance circuit obtained by feeding this nonlinear resistor with a negative resistance converter that is the Chua diode used in the JFET-based Liénard Oscillator circuit. The Schottky diode bridge in Figure 3 is used to achieve symmetry in the v-i characteristic of the Chua diode. In Figure 3, the complete nonlinear resistor circuit used in this study is also given.

A Chua diode has a piecewise linear (PWL) characteristic as shown in Figure 5. This characteristic consists of three segments. B_p is is the breakpoint voltage, and m_0 and m_1 are the slopes of the different regions of the characteristic shown in Figure 5 [24].

There are two reasons why Schottky diodes are used in this study. The first one is that they are usually preferred in the construction of the high-speed oscillators due to their low threshold voltages and fast switching. Therefore, the Schottky diodes are widely used in computer and radio frequency circuits. In this study, 1N5819 Schottky diodes are used. Figure 6 shows the v-i characteristic of this diode at 25 °C [25]. The second reason is to obtain the odd v-i characteristic of the PWL Chua diode given in Figure 5.

The v-i characteristic of the BF245 JFET used in this study can be seen in Figure 7 [26]. The *G* and *S* terminals of the JFET are connected to each other, i.e. V_{GS} voltage of the JFET is zero. Therefore, the upper curve, the curve obtained

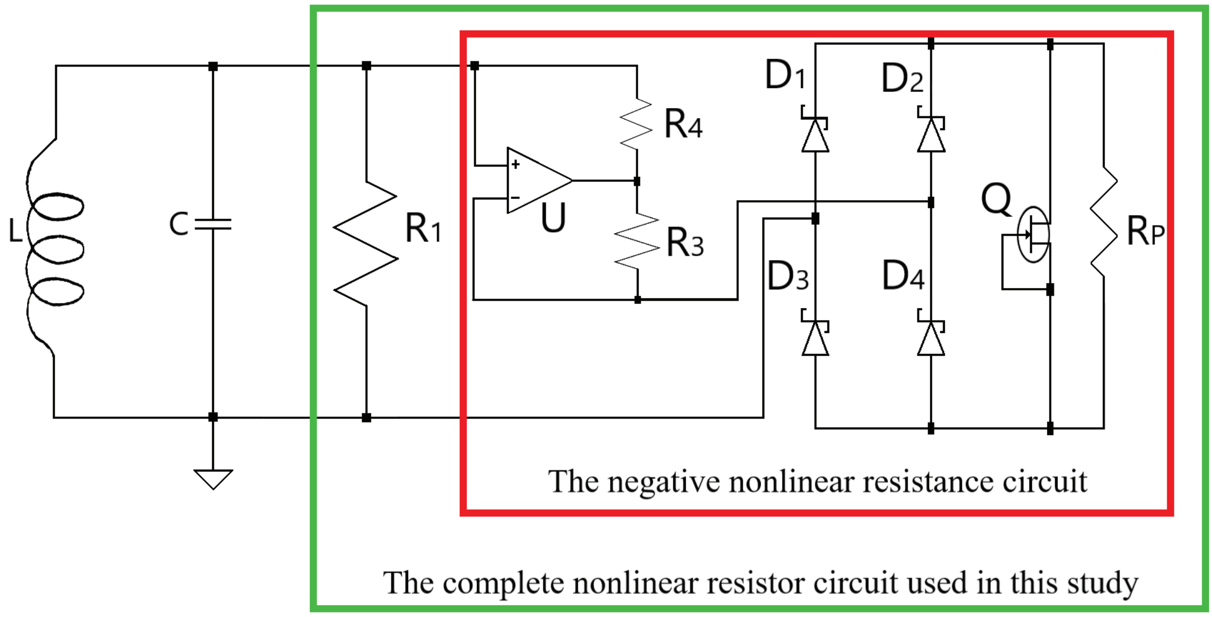

Figure 4. The Schottky diode bridge and the JFET-based Liénard Oscillator.

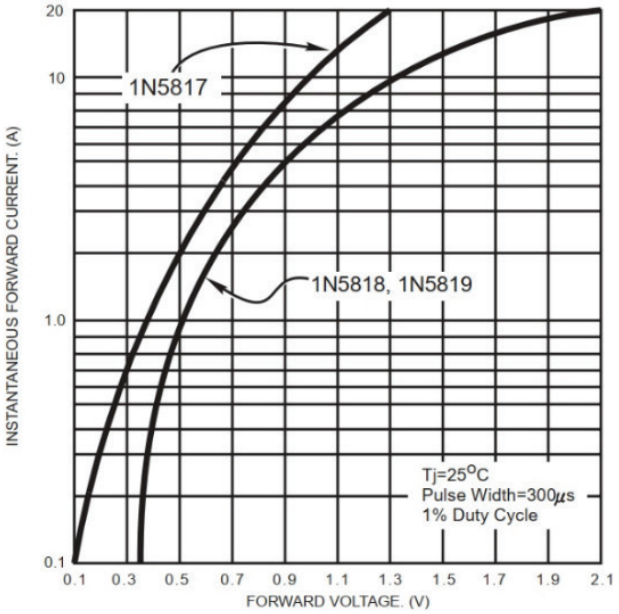

Figure 6. The v-i characteristic of 1N5819 Schottky diode at 25 °C[25].

for V_{GS} = 0 Volt is used in the construction of the nonlinear resistor. In Figure 7, it can be seen that the BF245 JFET in the Ohmic operating region can provide the average value of m_1 slope, but it is seen that the characteristic of the BF245 JFET does not have a slope big enough in the saturation region since its current is almost constant. The Schottky diode bridge feeding the BF245 JFET provides the odd function needed in Figure 5. However, the slope m_0 shown in Figure 5 is not obtained yet.

A resistor R_p placed in parallel with BF245 JFET is used to obtain the required slope m_0 since the v-i characteristics of a resistor is linear for a constant temperature. R_p The v-i

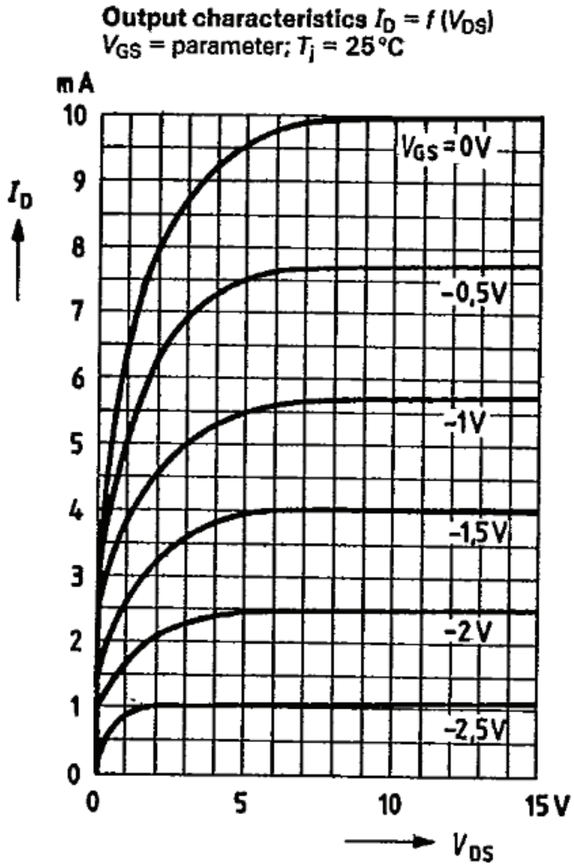

Figure 7. The v-i characteristic of the BF245 JFET [26].

characteristics of the resistor R_p in black, the BF245 JFET for V_{GS} = 0 Volt in red, and their equivalent resistor in blue are shown in Figure 8. Therefore, m_0 slope of the Chua diode is obtained with the resistor R_p and can be seen in the characteristic given Figure 8.

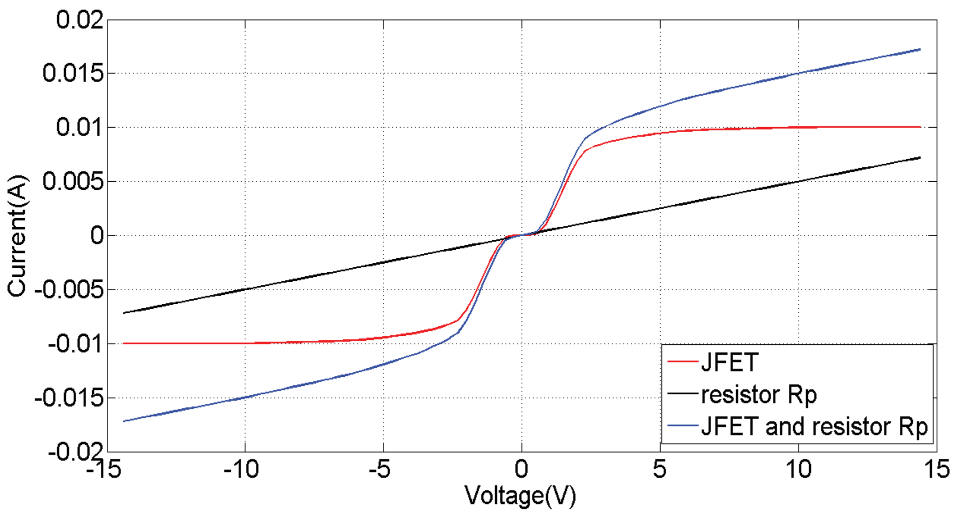

Figure 8. The v-i characteristics of the resistor R_p, BF245 JFET and the resistor R_p with BF245 JFET in the Chua diode.

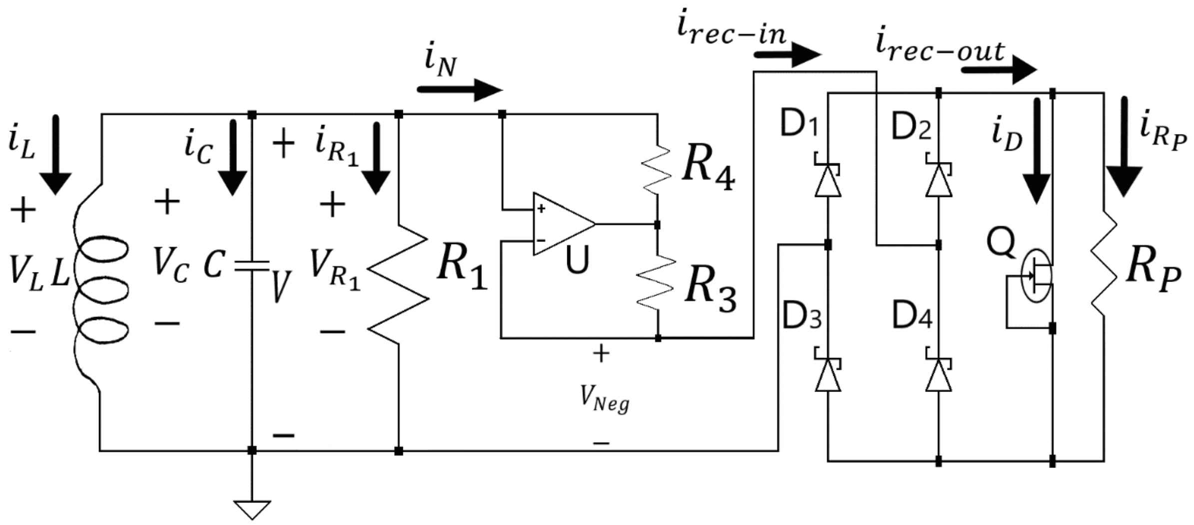

Figure 9. Representation of the currents and voltages of the circuit.

SCHOTTKY DIODE BRIDGE AND DYNAMIC MODEL OF JFET-BASED LIÉNARD OSCILLATOR CIRCUIT

In this section, the dynamic model of the Liénard Oscillator Circuit is derived. Figure 9 shows the polarities the currents and voltages of the circuit drawn for the analysis of the proposed oscillator in this study. Considering the circuit elements connected in parallel with each other, the voltages of the capacitor, inductor, resistor R_1 and the non-linear resistor are the same:

$$V = V_c = V_L = V_N = V_{R_1} = V_{Neg} \tag{8}$$

The current of a JFET is given as

$$i_D = K\left((V_{GS} - V_T)V_{DS} - \frac{(V_{DS})^2}{2}\right) \tag{9}$$

The current of a JFET operating in the saturation region:

$$i_{sat} = G_{sat}V_{sat} = G_{sat}V_{Dsat} \tag{10}$$

where i_{sat} is the saturation current and G_{sat} is the saturation conductivity of the JFET.

Since the gate and source terminals of the JFET are connected to each other, $V_{GS} = 0$ Volts. In a saturated JFET, the following is true:

$$V_{DS} = V_{DSsat} = V_{GS} - V_T = -V_T \tag{11}$$

and

$$i_D = K\frac{(V_T)^2}{2} \tag{12}$$

The saturation current of the JFET shown in Figure 8 is an important parameter. By adding the resistor R_p in parallel to the JFET, the PWL Chua diode v-i characteristic (The breaking point B_P, the slope m_0, and the slope m_1) shown in Figure 5 is obtained and, therefore, the oscillator circuit shown in Figure 5 can be made. Breaking point voltage in Figure 5 can be taken as.

$$B_P = V_{DSsat} \tag{13}$$

The output current of the Schottky diode bridge is the sum of the JFET and the R_p resistor:

$$i_{rec-out} = i_D + i_{R_P} \tag{14}$$

The input current of the Schottky diode bridge can be calculated considering the direction of the voltage applied to the Schottky diode bridge:

$$i_{rec-in} = sign(V) \cdot i_{rec-out} \tag{15}$$

Input current of negative resistance converter circuit is given as

$$i_{Neg} = g_N V_{Neg} = -V_{Neg}\frac{R_3}{R_2 * R_4} \tag{16}$$

If $R_3 = R_4$, this current turns into

$$i_{Neg} = g_N V_{Neg} = -\frac{V_{Neg}}{R_2} \tag{17}$$

The Chua diode current due to negative resistance converter circuit is given as

$$i_N = -sign(V) \cdot i_{rec-out} \tag{18}$$

Total current of the equivalent nonlinear negative resistor is given as

$$i_{N_R} = i_{R_1} + i_N \tag{19}$$

The current of the linear time-invariant (LTI) inductor and the current of the LTI capacitor respectively can be given as

$$i_L = \frac{1}{L}\int_0^t V_L\, dt + i_L(0) \tag{20}$$

and

$$i_c = C\frac{dV_C}{dt} \tag{21}$$

The piecewise linear function of the Chua diode current is given as

$$i_N = g(V_{N_R}) = m_0 V_{N_R} + \frac{m_1 - m_0}{2}\left(|V_{N_R} + B_p| - |V_{N_R} - B_p|\right) \tag{22}$$

The current of the Chua diode is also given in the following form:

$$i_N = g(V) = \begin{cases} m_1(V - B_p) + B_p,\ B_p \le V \\ m_0 V\ ,-B_p \le V \le B_p \\ m_1(V + B_p) - B_p,\ V \le -B_p \end{cases} \tag{23}$$

Input current of the negative resistance converter circuit is

$$i_N = g_N V \tag{24}$$

where g_N is the conductivity of the negative resistance.

Since $V = V_c = V_L = V_N = V_{R1} = V_{Neg}$, the conductance of the negative resistance converter circuit can be obtained as

$$g_N = \frac{i_N}{V} = \begin{cases} m_1 + \frac{B_p(-m_1+1)}{V} & ,\ B_p \le V_{N_R} \\ m_0 & ,-B_p \le V_{N_R} \le B_p \\ m_1 + \frac{B_p(m_1-1)}{V} & ,\ V_{N_R} \le -B_p \end{cases} \tag{25}$$

If the slopes m_0 and m_1 shown in Figure 5 are calculated:

$$m_0 = \frac{1}{R_P} \tag{26}$$

and

$$m_1 \cong -G_{sat} - \frac{1}{R_P} \tag{27}$$

If Kirchoff's Current Law of is used:

$$i_C + i_{R_1} + i_N + i_L = 0 \tag{28}$$

For $B_p \le V$, the Equation (28) turns into

$$C\,\frac{dV}{dt} + \left(\frac{V}{R_1} + m_1(V - B_p) + B_p\right) + \frac{1}{L}\int_0^t V\,dt + i_L(0) = 0 \tag{29}$$

For $V \le B_p$, the Equation (28) turns into

$$C\,\frac{dV}{dt} + \left(\frac{V}{R_1} + m_0(V + B_p) - B_p\right) + \frac{1}{L}\int_0^t V\,dt + i_L(0) = 0 \tag{30}$$

By taking the derivative of Equation (29) and rearranging them, the following equation is obtained:

$$C\,\frac{d^2V}{dt^2} + \left(\frac{1}{R_1} + m_1\right)\frac{dV}{dt} + \frac{1}{L}V = C\,\frac{d^2V}{dt^2} + \left(\frac{1}{R_1} - G_{sat} - \frac{1}{R_P}\right)\frac{dV}{dt} + \frac{1}{L}V = 0 \tag{31}$$

If Equation (30) is rearranged for $-B_p \le V_{Neg} \le B_p$ and after taking its derivative, the following equation is obtained as

$$\frac{d^2V}{dt^2} + \frac{1}{C}\left(\frac{1}{R_1} + m_0\right)\frac{dV}{dt} + \frac{1}{LC}V = \frac{d^2V}{dt^2} + \frac{1}{C}\left(\frac{1}{R_1} - \frac{1}{R_p}\right)\frac{dV}{dt} + \frac{1}{LC}V = 0 \tag{32}$$

Equations (31) and (32) are differential equations together that describe the dynamics of this circuit. From these equations it can be seen that the circuit is a Liénard Oscillator. Its simulation is to be carried out in the next section.

SIMULATION OF SCHOTTKY DIODE BRIDGE AND JFET-BASED LIÉNARD OSCILLATOR

The Liénard Oscillator proposed in this study shown in Figure 9 is simulated with LTspice in this section. The LTspice circuit diagram of the Liénard Oscillator is shown in Figure 10. The parameters used in the simulation are given in Table 1. The values of the resistors R_3 and R_4 are taken as equal. The simulation results of the circuit are given in Figures 11 to 20.

Although the voltage of the circuit in periodic steady-state given in Figure 11 resembles a sinusoidal wave with respect to time, it is seen that the peak value of the wave is pointier than a sinusoidal wave.

Table 1. Parameters of the Liénard Oscillator circuit

Circuit Parameter	Value
C	10 nF
L	1 mH
R_1	2 kOhm
R_3	1 kOhm
R_4	1 kOhm
R_p	2 kOhm
G_{sat}	1mS
V_T	-10 V
B_p	6 V
K	0,0002

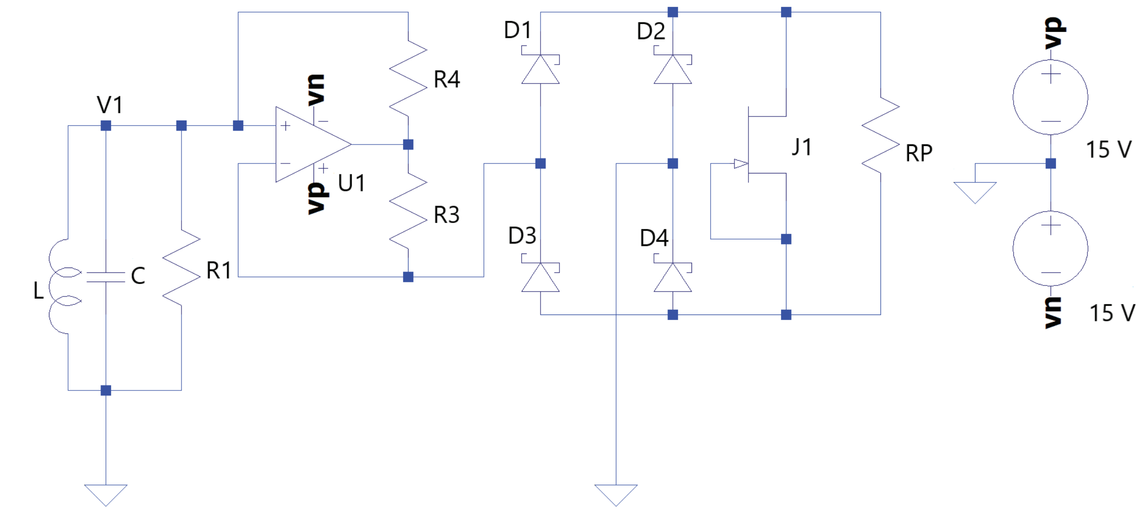

Figure 10. LTspice Modeling of Schottky diode bridge and JFET based Liénard Oscillator circuit.

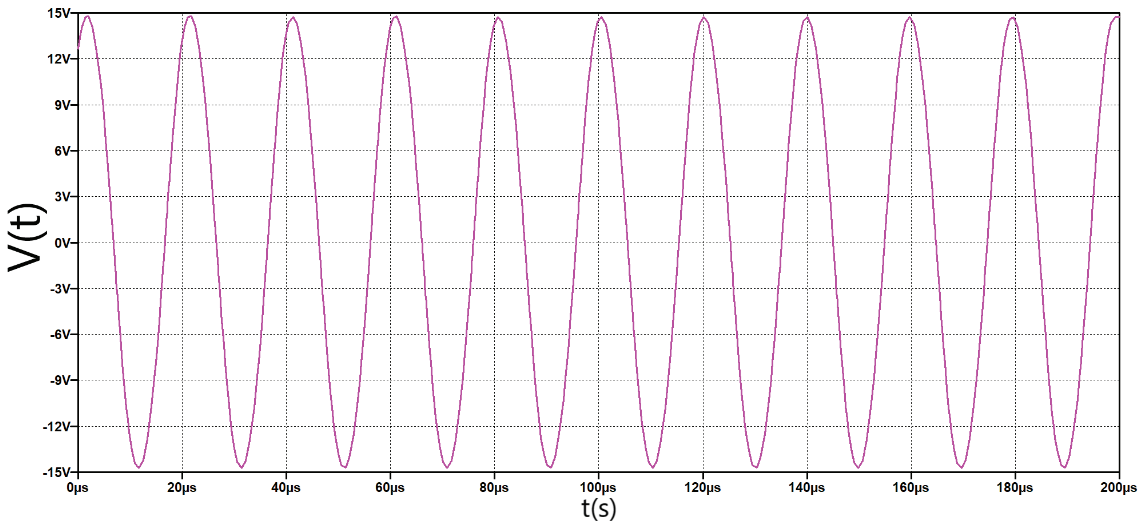

Figure 11. Voltage of the oscillator circuit.

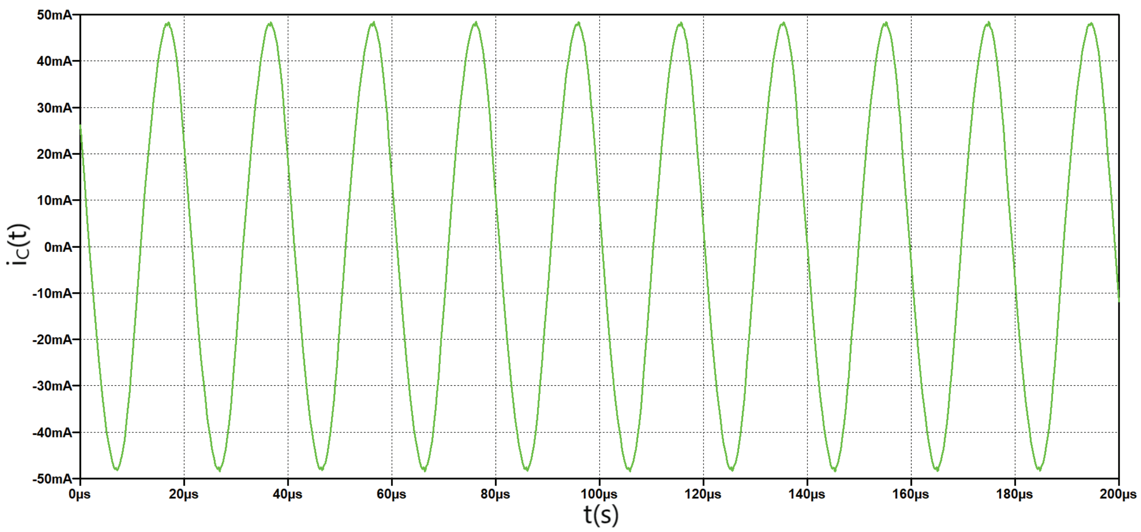

Figure 12. Current of the circuit capacitor at periodic steady state.

The current of the circuit capacitor at periodic steady state is not a sinusoidal waveform and has tapered peaks as shown in Figure 12.

The effect of the threshold voltage of the Schottky diodes, that is the zero-crossing distortion, can be seen in Figure 13 when the current of the Chua diode passes through zero in the periodic steady state.

It can be seen in Figure 14 that a large second harmonic does exist in the equivalent nonlinear resistor current in the periodic steady state. Due to this feature, that is the second harmonic generation, this Chua diode has been used in the construction of the chaotic circuit in [20].

The inductor current is not sinusoidal and a triangular distortion is observed in the peak of the signal in the periodic steady state as shown in Figure 15.

The limit cycle of the capacitor in Figure 16 resembles an ellipse.

In Figure 17, it can be seen that the v-i characteristic of the Chua diode is an odd function, since it is symmetric with respect to the origin, and shows a negative resistance feature since it is only in the second and fourth quadrants due to the negative resistance convertor. The effect of the Schottky diode thresholds can be seen in Figure 17. In our opinion, also the effect of the reverse recovery current of

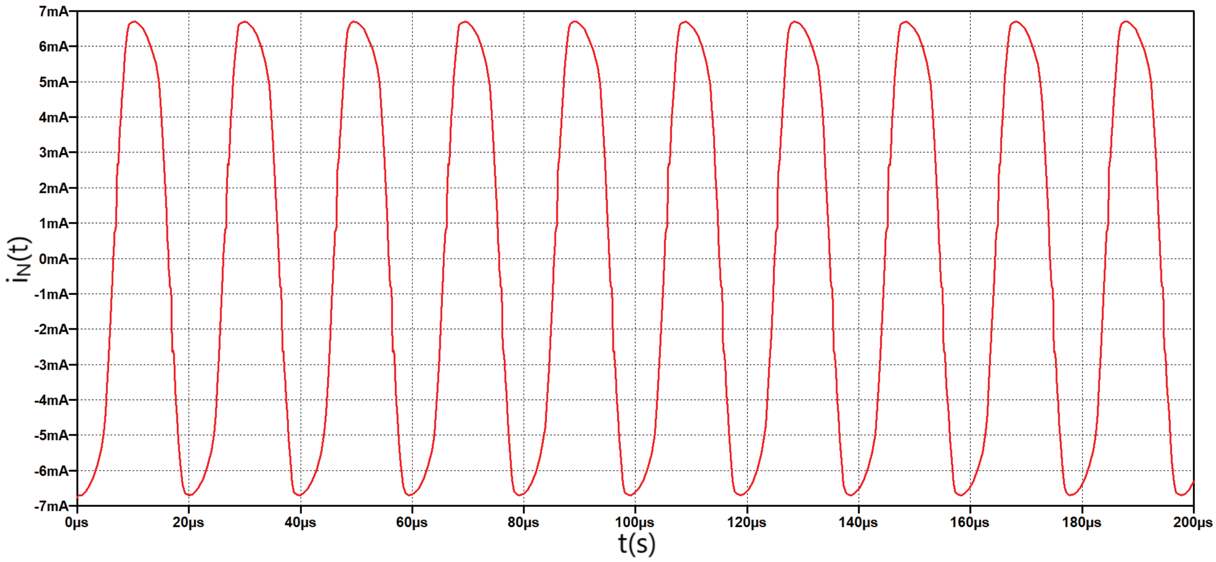

Figure 13. Current of Chua diode in the circuit at periodic steady state.

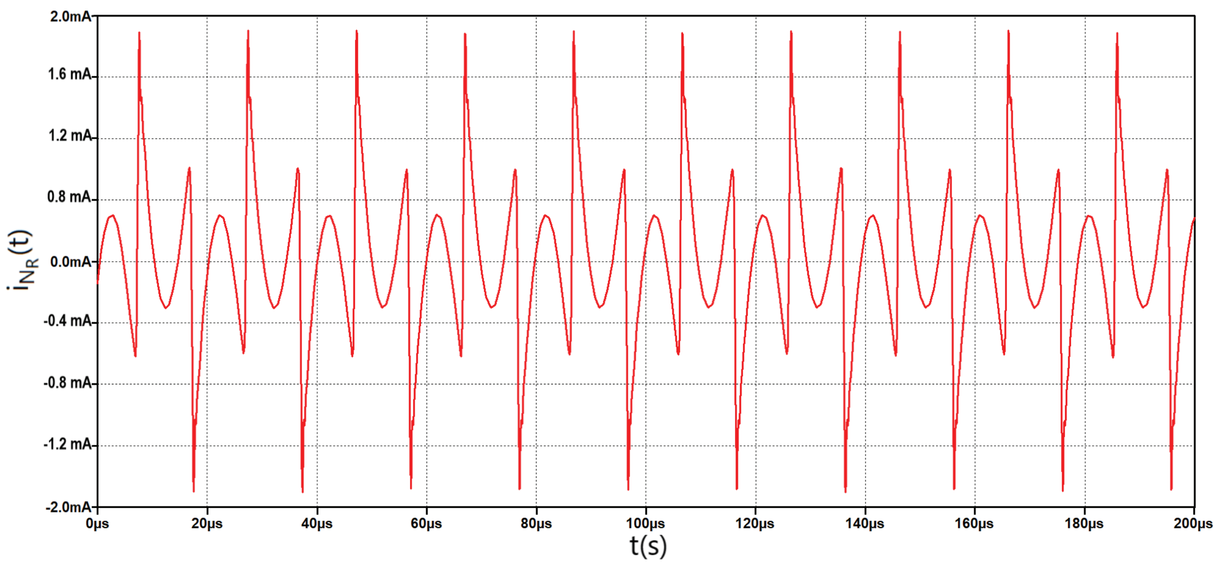

Figure 14. Current of the equivalent resistor in the periodic steady state.

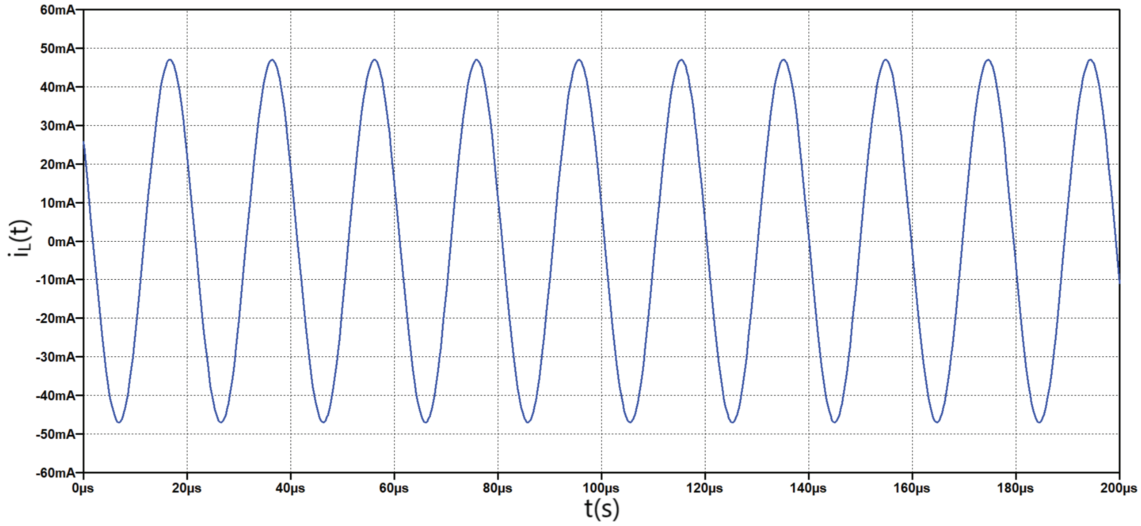

Figure 15. Current of the circuit inductor in periodic steady state.

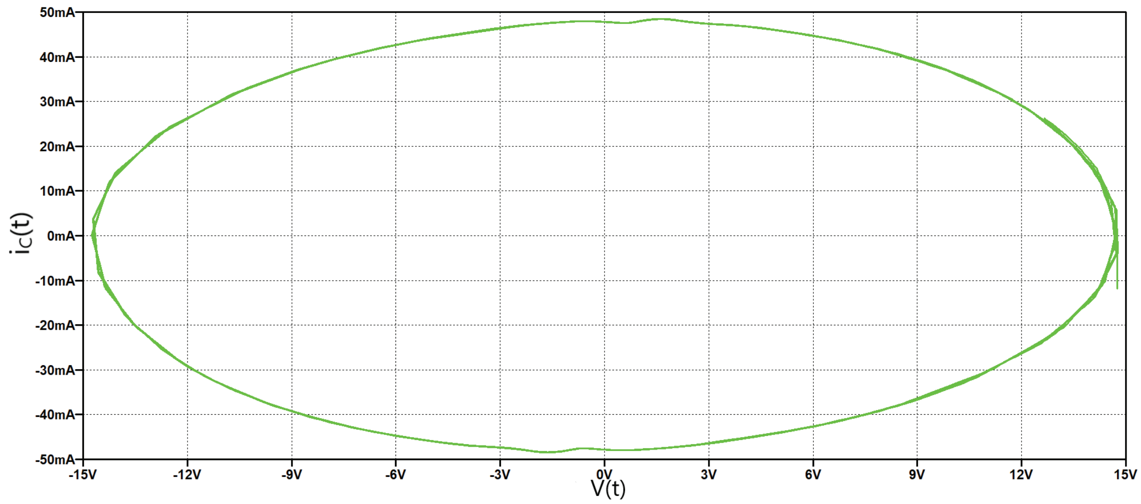

Figure 16. Limit cycle of capacitor.

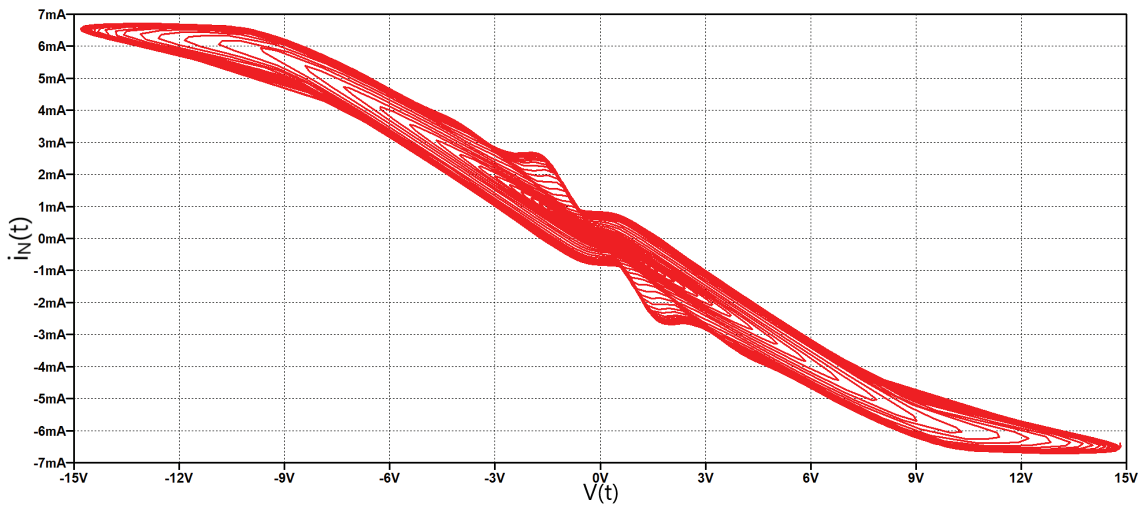

Figure 17. v-i characteristic of Chua diode.

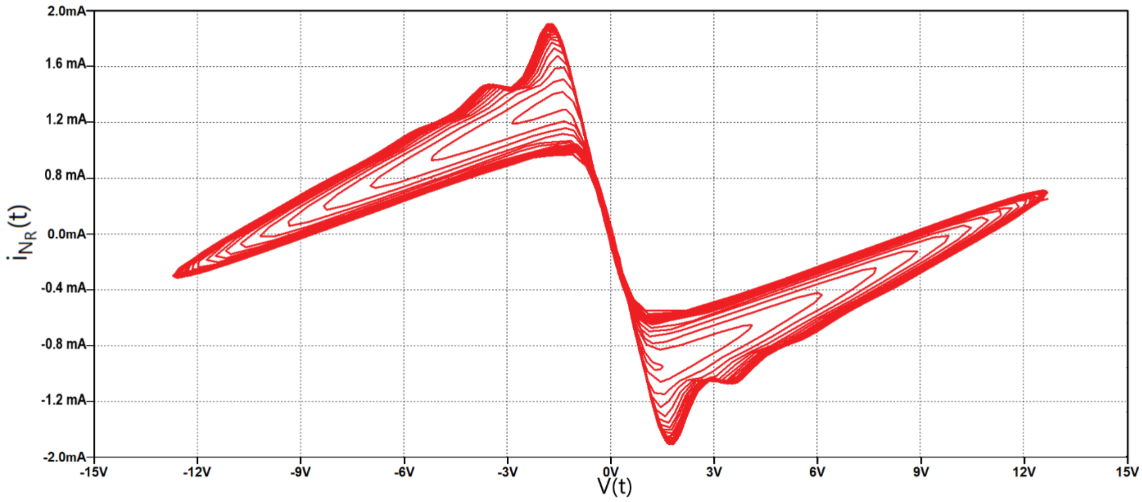

Figure 18. The v-i characteristic of the equivalent resistance in the circuit.

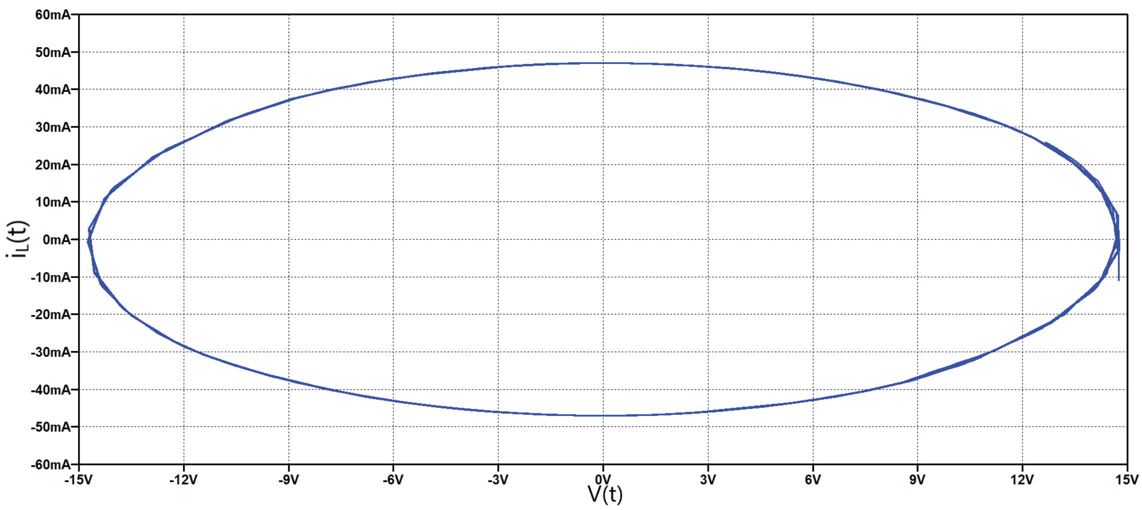

Figure 19. Limit cycle of inductor.

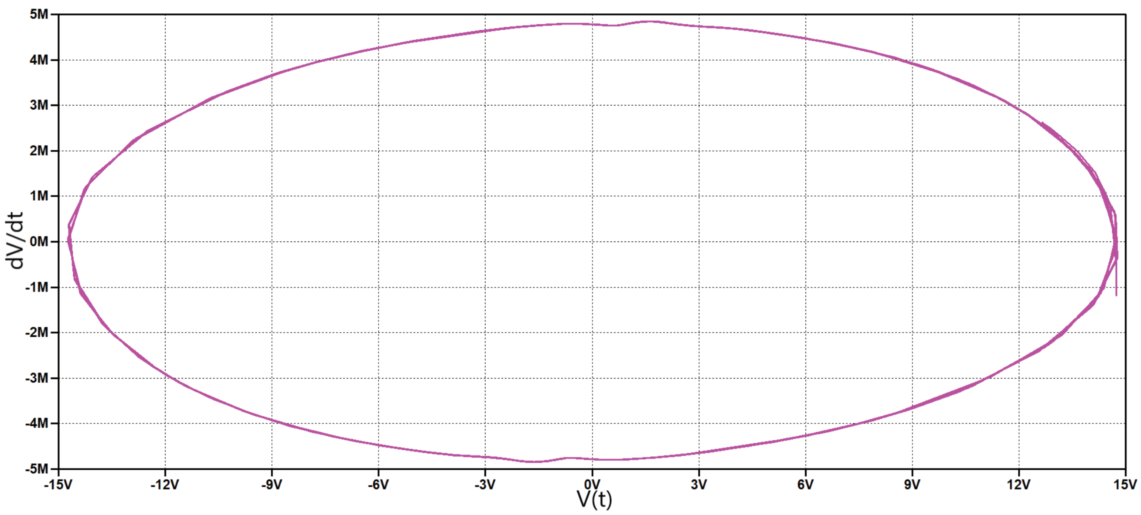

Figure 20. Limit cycle or the phase portrait of the Liénard Oscillator.

the diodes on v-i characteristic of Chua diode can be seen in Figure 17.

From the v-i characteristic of the equivalent resistance of the circuit given in Figure 18, it can be seen that the characteristic is an almost cubic function. It is also symmetric with respect to the origin and also shows a negative resistance feature since it is only in the second and fourth quadrants due to the negative resistance convertor. The curve almost looks like a negative cubic function and it can be shown to be so using McLaurin series and taking as the first two nonzero terms as done for the Van der Pol Oscillator in [9]. In our opinion, also the effect of the reverse recovery current of the diodes on v-i characteristic of Chua diode can be seen in Figure 18.

The limit cycle of the inductor in Figure 19 resembles an ellipse as the limit cycle of the capacitor also does as in Figure 16.

The limit cycle or the phase portrait in Figure 20 also resembles an ellipse.

CONCLUSION

The Liénard Oscillator can be implemented with various circuit elements. In this study, a Chua diode consisting of a Schottky diode bridge and a JFET is used to obtain the nonlinear resistance in the Liénard Oscillator. By using the circuit equations, it is proven that it is a Liénard Oscillator. It is also shown that the Schottky diode bridge, which feeds the JET provides an odd function or the even nonlinear resistance required for a Liénard Oscillator easily and can be used with other semiconductor circuit elements in the future to make other variants of the Liénard Oscillator. The circuit analysis and how to obtain the odd function of the Liénard oscillator are given in detail so that the other researchers can go through the necessary tasks easily for other Lienard Oscillator topologies. The oscillator's simulation is done using LTspice program. The limit cycle of the circuit, currents and voltages of the circuit elements are obtained from the simulations. Having periodic waveforms and limit cycles, the proposed circuit is shown to operate as a Liénard Oscillator. In the Liénard Oscillator proposed in this study, it is provided that $V_{GS} = 0$ Volt in JFET, but if the voltage V_{GS} is made variable using a voltage divider circuit or an adjustable power supply, the characteristic of the Chua diode changes, and an adjustable Liénard Oscillator can be obtained.

VDPO is a subset of Liénard Oscillator and, even, it does not have any analytical solutions. Neither do most of Liénard Oscillators. Perhaps, a series solution or an approximate solution for such a system can also be done. Since there is not an equation describing how the oscillator frequency is affected by the circuit elements, a parametric study, which could be done, would increase the number of simulations given in this study. However, these can be the subject of future studies due to space considerations.

AUTHORSHIP CONTRIBUTIONS

Authors equally contributed to this work.

DATA AVAILABILITY STATEMENT

The authors confirm that the data that supports the findings of this study are available within the article. Raw data that support the finding of this study are available from the corresponding author, upon reasonable request.

CONFLICT OF INTEREST

The author declared no potential conflicts of interest with respect to the research, authorship, and/or publication of this article.

ETHICS

There are no ethical issues with the publication of this manuscript.

REFERENCES

[1] Van der Pol B. A theory of the amplitude of free and forced triode vibrations. Radio Review (London) 1920;1:754−762.

[2] Van der Pol B. LXXXVIII. On "relaxation-oscillations." London Edinburgh Philos Mag J Sci 1926;2:978−992. [CrossRef]

[3] Van der Pol B, van der Mark J. Frequency demultiplication. Nature 1927;120:363−364. [CrossRef]

[4] Van der Pol B. The nonlinear theory of electric oscillations. Proceed Inst Radio Eng 1934;22:1051−1086. [CrossRef]

[5] Liénard A. Etude des oscillations entretenues. Rev Gen Electr (France) 1928;23:901−912, 946−954.

[6] Nagumo J, Arimoto S, Yoshizawa S. An active pulse transmission line simulating nerve axon. Proceed IRE 1962;50:2061−2070. [CrossRef]

[7] Dinh TP, Demongeot J, Baconnier P, Benchetrit G. Simulation of a biological oscillator: the respiratory system. J Theor Biol 1983;103:113−132. [CrossRef]

[8] Atlas GM, Desiderio MC. Solutions to the Van der Pol equation: a model of aortic blood flow. IEEE. In Proceedings of the IEEE 32nd Annual Northeast Bioengineering Conference,IEEE 2006:143−144.

[9] Han M. Bifurcation Theory of Limit Cycles. Beijing: Science Press; 2013.

[10] Slight TJ, Romeira B, Wang L, Figueiredo JM, Wasige E, Ironside CN. A Liénard oscillator resonant tunnelling diode-laser diode hybrid integrated circuit: model and experiment. IEEE J Quantum Electron 2008;44:1158−1163. [CrossRef]

[11] Kingston SL, Kapitaniak T. Rich dynamics of memristor based Liénard systems. . In Mem-Elements for

Neuromorphic Circuits with Artificial Intelligence Applications. New York: Academic Press; 2021. p. 125−145. [CrossRef]

[12] Çakır K, Mutlu R, Karakulak E. Ters-Paralel Bağlı Schottky Diyot Dizisi Tabanlı Van der Pol Osilatörü Devresinin Modellenmesi ve LTspice ve Simulink Kullanarak Analizi. EMO Bilimsel Dergi 2021;11:81−91.

[13] Doutetien EA, Yehossou AR, Mallick P, Rath B, Delphin Monsia M. On the General Solutions of a Nonlinear Pseudo-Oscillator Equation and Related Quadratic Liénard Systems. Proceed Indian Nat Sci Acad 2020;86:154987. [CrossRef]

[14] Akplogan ARO, Adjaï KKD, Akande J, Avossevou GYH, Monsia MD. Modified Van der Pol-Helmholtz oscillator equation with exact harmonic solutions Res Sq 2022. [Epub ahead of print]. doi: 10.21203/rs.3.rs-1229125/v1 [CrossRef]

[15] Chandrasekar VK, Senthilvelan M, Lakshmanan M. Unusual Liénard-type nonlinear oscillator. Phys Rev E 2005;72:066203. [CrossRef]

[16] Tuna SE. Synchronization analysis of coupled Lienard-type oscillators by averaging. Automatica 2012:1885−1891. [CrossRef]

[17] Sun X. Multiple limit cycles of some strongly nonlinear Liénard-Van der Pol oscillator. Appl Math Comput 2015;270:620−630. [CrossRef]

[18] Kpomahou YJF, Adéchinan JA. Nonlinear dynamics and active control in a liénard-type oscillator under parametric and external periodic excitations. Am J Comput Appl Math 2020;10:48−61.

[19] Gubbiotti G, Nucci MC. Noether symmetries and the quantization of a Lienard-type nonlinear oscillator. J Nonlinear Math Phys 2014;21:248−264. [CrossRef]

[20] Sinelshchikov DI. Nonlocal deformations of autonomous invariant curves for Liénard equations with quadratic damping. Chaos Solit Fract 2021;152:111412. [CrossRef]

[21] Bhattacharyya S, Ghosh A, Ray DS. Microscopic quantum generalization of classical Liénard oscillators. Phys Rev E 2021;103:012118. [CrossRef]

[22] Deka JP, Sarma AK, Govindarajan A, Kulkarni M. Multifaceted nonlinear dynamics in PT-symmetric coupled Liénard oscillators. Nonlinear Dyn 2020;100:1629−1640. [CrossRef]

[23] Karayaka Ü, Alakuş C, Mutlu R, Karakulak E. Making Chua's Diode With A Schottky Diode-Bridge-Fed Jfet Mosfet. Trakya Üniv Mühendislik Bilim Derg 2021;22:41−50.

[24] Kennedy MP. Robust OP Amp realization of Chua's circuit. Frequenz 1992;46. [CrossRef]

[25] 1N5819 Datasheet(PDF) - Shenzhen Luguang Electronic Technology Co., Ltd n.d. https://www.alldatasheet.com/datasheet-pdf/pdf/479637/LUGUANG/1N5819.html (Accessed on Feb 22, 2022).

[26] BF245 pdf, BF245 Description, BF245 Datasheet, BF245 view ::: ALLDATASHEET ::: n.d. https://pdf1.alldatasheet.com/datasheet-pdf/view/44472/SIEMENS/BF245.html (Accessed on Apr 30, 2022).